
Princeton Plasma Physics Laboratory

PPPL-

PPPL-



Prepared for the U.S. Department of Energy under Contract DE-AC02-09CH11466.

Princeton Plasma Physics Laboratory

Report Disclaimers

Full Legal Disclaimer

This report was prepared as an account of work sponsored by an agency of the United States Government. Neither the United States Government nor any agency thereof, nor any of their employees, nor any of their contractors, subcontractors or their employees, makes any warranty, express or implied, or assumes any legal liability or responsibility for the accuracy, completeness, or any third party's use or the results of such use of any information, apparatus, product, or process disclosed, or represents that its use would not infringe privately owned rights. Reference herein to any specific commercial product, process, or service by trade name, trademark, manufacturer, or otherwise, does not necessarily constitute or imply its endorsement, recommendation, or favoring by the United States Government or any agency thereof or its contractors or subcontractors. The views and opinions of authors expressed herein do not necessarily state or reflect those of the United States Government or any agency thereof.

Trademark Disclaimer

Reference herein to any specific commercial product, process, or service by trade name, trademark, manufacturer, or otherwise, does not necessarily constitute or imply its endorsement, recommendation, or favoring by the United States Government or any agency thereof or its contractors or subcontractors.

PPPL Report Availability

Princeton Plasma Physics Laboratory:

<http://www.pppl.gov/techreports.cfm>

Office of Scientific and Technical Information (OSTI):

<http://www.osti.gov/bridge>

Related Links:

[U.S. Department of Energy](#)

[Office of Scientific and Technical Information](#)

[Fusion Links](#)

Geometric phases of the Faraday rotation of electromagnetic waves in magnetized plasmas*

Jian Liu¹ and Hong Qin^{1,2}

¹*Department of Modern Physics, University of Science and Technology of China, Hefei, Anhui 230026, China*

²*Plasma Physics Laboratory, Princeton University, Princeton, New Jersey 08543, USA*

Abstract

The geometric phase of circularly polarized electromagnetic waves in nonuniform magnetized plasmas is studied theoretically. The variation of the propagation direction of circularly polarized waves results in a geometric phase, which also contributes to the Faraday rotation, in addition to the standard dynamical phase. The origin and properties of the geometric phase is investigated. The influence of the geometric phase to plasma diagnostics using Faraday rotation is also discussed as an application of the theory.

The geometric phase is a ubiquitous phenomenon in almost all subfields of physics [1–16]. Early in 1958, Spitzer anticipated its existence when inventing the figure-8 stellarator [17]. In 1984, M. Berry discovered the famous Berry phase in quantum adiabatic systems [3]. Soon Hannay brought forward the Hannay’s angle in the context of classical mechanics [18], and Simon discussed the geometric phase through a more abstract viewpoint of mathematics [19]. In plasma physics, the geometric phase associated with gyrophase has been studied [20–22], offering a deeper insight into the modern gyrokinetic theory. In this paper we discuss another geometric phase phenomenon in plasma physics, the geometric phase of the Faraday rotation of electromagnetic (EM) waves in magnetized plasmas.

The Faraday rotation effect is a magneto-optical phenomenon first discovered by Faraday in 1845. It describes the change of the polarization direction of a linearly polarized EM wave when propagating parallel to the background magnetic field in a magnetized medium. The linearly polarized EM wave can be expressed as the linear superposition of two circularly polarized characteristic waves, a right circularly polarized and a left circularly polarized wave [see Eq. (23)]. The polarization orientation of the linearly polarized wave is determined by the phase difference of the two circularly polarized waves [see Eq. (23)]. Because of the existence of the background magnetic field, the right and left circularly polarized waves have different dispersion relations, which induce a phase difference for the linearly polarized wave increasing along the wave trajectory.

For a wave propagating in a general direction, if its frequency is high enough compared with the electron gyrofrequency and it propagates not too close to the perpendicular direction, the two characteristic waves are still circularly polarized [23]. Thus, the analysis on the Faraday effect based on two circularly polarized characteristic waves is also valid in this case.

When propagating in inhomogeneous, magnetized plasmas, in addition to the normal dynamical phase, a circularly polarized wave may also contain a geometric phase. Because of the inhomogeneity, the propagation directions of EM waves vary from place to place. In addition, the surfaces, in which the polarization orientations reside, rotate correspondingly. As a result of the rotation, there appears an additional geometric phase which doesn’t evolve according to the dispersion relations. It contributes to the Faraday rotation angle as well (See Fig. 1).

In laboratory plasma experiments, diagnostic methods have been proposed to probe plas-

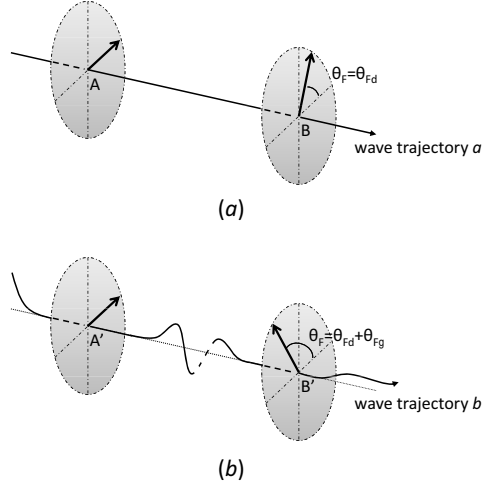


FIG. 1. Illustration of a linearly polarized EM wave propagates through a magnetized medium. If the magnetized medium is homogeneous, the wave trajectory is straight as in figure (a). The Faraday rotation angle θ_F contains only the dynamical part θ_{Fd} , which is determined by the difference of the dispersion relations of right and left circularly polarized waves. If the wave propagates in nonuniform magnetized plasmas, its trajectory is a curve and may twist as in figure (b), the Faraday rotation angle contains an additional geometric part θ_{Fg} , which relies on the spatial geometric structure of the wave vector. The bold line and curve indicate trajectories of waves, and the black arrows on the polarization plane indicate the waves' polarization directions of the linearly polarized wave.

ma properties through the Faraday rotation, such as the plasma density and the poloidal fields in tokamaks [24–31]. In the last part of this paper, we will estimate the influence of the geometric phase on plasma diagnostics and propose some possible schemes to measure the geometric Faraday rotation angle experimentally.

Through this paper, the background magnetic field is denoted by \mathbf{B}_0 , the complex perturbed fields with a specific frequency ω after time-domain Fourier transform as \mathbf{B} and \mathbf{E} , and their complex amplitudes as $\tilde{\mathbf{B}}$ and $\tilde{\mathbf{E}}$.

First, we give a general description of the geometric phase associated with the Faraday rotation. The waves in a uniformly magnetized cold plasma can be treated by the standard method [32]. However, almost all real magnetized plasmas, both in laboratory and space plasmas, are spatially nonuniform. In many cases, the nonuniformity is weak in the sense that the space scale of the nonuniformity of background field $L_{B_0} = B_0/\nabla B_0$ is much

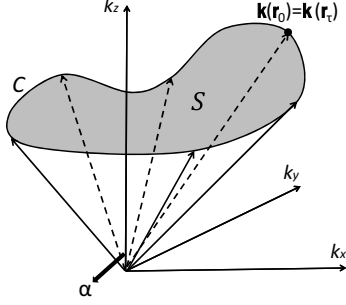


FIG. 2. When the wave-vector $\mathbf{k}_d(\mathbf{r})$ returns its original position in the parameter space composed of (k_x, k_y, k_z) , its path forms a closed loop C . Here, S denotes the surface enclosed by C . The magnitude of the type-I geometric phase of the circular polarized wave, and hence the corresponding type-I geometric Faraday rotation angle, is equal to the solid angle α spanned by C . The geometric phases of right and left circularly polarized waves have opposite signs.

larger than the wave length λ , *i.e.*, $\varepsilon \equiv \lambda/L_{B_0} \ll 1$. The analyses in this paper focus on EM waves propagating in such weakly inhomogeneous magnetized plasmas. The weak nonuniformity may bring a small deviation to the wave propagation direction. At the same time, the phase of circularly polarized waves in nonuniform magnetized plasmas contains an additional geometric part θ_g besides the familiar dynamical phase $\theta_d = \int_P \mathbf{k}_d \cdot d\mathbf{r} - \omega t$ defined by the wave's frequency and the local dispersion relation $\mathbf{k}_d = \mathbf{k}_d(\omega, \mathbf{B}_0(\mathbf{r}))$ along the wave trajectory P . The geometric phase can be expressed as $\theta_g = \int_P \mathbf{k}_g \cdot d\mathbf{r}$ for some wave vector \mathbf{k}_g [see Eq. (15)] resulting from the variation of the wave's polarization surface. As its name implies, the geometric phase has a deep geometric origin, and depends only on the geometric property of the wave vector, instead of the wave's frequency and other plasma parameters. The geometric phase θ_g can be further divided into two parts, the type-I geometric phase θ_{gI} and the type-II geometric phase θ_{gII} . Similar to the Berry phase in quantum physics, the type-I geometric phase θ_{gI} comes from the inevitable rotation of the frame because of the non-commutativity of spatial rotation operations, which corresponds to the Rytov law [33]. If the dynamical part of the wave vector \mathbf{k}_d returns to its origin value after the wave travels a distance, the magnitude of θ_{gI} equals exactly the solid angle spanned by the closed path of the wave vector \mathbf{k}_d in the parameter space (see Fig. 2). On the other hand, the type-II geometric phase θ_{gII} originates from the non-inertial frame effect caused by the rotation of the polarization surface.

Now we give a theoretical derivation of the geometric phase θ_g by considering a circularly polarized EM wave propagating in a magnetized plasma. If the background field is both spatially and temporally uniform, the wave equation in the Fourier space is

$$\mathbf{k} \times \mathbf{k} \times \mathbf{E} + \frac{\omega^2}{c^2} \boldsymbol{\epsilon}_r \cdot \mathbf{E} = 0 , \quad (1)$$

where $\boldsymbol{\epsilon}_r$ is the relative permittivity tensor determined by the properties of the magnetized plasma. Dispersion relations can be obtained from Eq. (1). For the parallel propagating right circularly polarized (R) wave and left circularly polarized (L) wave in a cold collisionless plasma, the dispersion relations can be written as

$$\mathbf{k}^2 = \frac{\omega^2}{c^2} \left[1 - \sum_s \frac{\omega_{ps}^2}{\omega(\omega \pm \Omega_s)} \right] \quad (2)$$

respectively, where ω_{ps} and Ω_s are the plasma frequency and gyrofrequency for particles of species s respectively. Following the standard convention in plasma physics, the right and left here are defined with respect to the background field. In a slightly spatially nonuniform magnetic field, we can only apply the Fourier analysis in the time-domain, and the wave equation becomes

$$\nabla \times \nabla \times \mathbf{E} - \frac{\omega^2}{c^2} \boldsymbol{\epsilon} \cdot \mathbf{E} = 0 . \quad (3)$$

Here, the EM perturbations are assumed to have the form

$$\mathbf{E}(\mathbf{r}, t) = \tilde{\mathbf{E}}(\mathbf{r}) e^{i[\theta(\mathbf{r}) - \omega t + \theta_0]} , \quad (4)$$

where the complex amplitude $\tilde{\mathbf{E}}(\mathbf{r})$ and $\theta(\mathbf{r})$ are both functions of the spatial coordinates \mathbf{r} .

If we define wave vector as

$$\mathbf{k} = \frac{d}{d\mathbf{r}} \theta(\mathbf{r}) , \quad (5)$$

then Eq. (3) can be rewritten as

$$\mathbf{k} \times \mathbf{k} \times \tilde{\mathbf{E}} + \frac{\omega^2}{c^2} \boldsymbol{\epsilon}_r(\mathbf{r}) \cdot \tilde{\mathbf{E}} = i \nabla \times (\mathbf{k} \times \tilde{\mathbf{E}}) + i \mathbf{k} \times (\nabla \times \tilde{\mathbf{E}}) + \nabla \times \nabla \times \tilde{\mathbf{E}} . \quad (6)$$

The wave vector \mathbf{k} can be split into two parts:

$$\mathbf{k} = \mathbf{k}_d + \mathbf{k}_g , \quad (7)$$

where \mathbf{k}_d is called the dynamical wave vector and it is defined by the local dispersion relation

$$\mathbf{k}_d \times \mathbf{k}_d \times \tilde{\mathbf{E}} + \frac{\omega^2}{c^2} \boldsymbol{\epsilon}_r(\mathbf{r}) \cdot \tilde{\mathbf{E}} = 0 . \quad (8)$$

Equation (8) has the same form as Eq. (1), but the relative permittivity tensor $\epsilon_r(\mathbf{r})$ is a slowly varying function of position now. The difference between \mathbf{k} and \mathbf{k}_d is defined to be the geometric wave vector \mathbf{k}_g .

In this paper, we focus on the circularly polarized characteristic waves determined by Eq. (8). It's familiar that in a homogeneous magnetized plasma there are two circularly polarized characteristic waves propagating parallel to the background field. In an inhomogeneous magnetized plasma, the wave cannot propagate exactly parallel to the background field everywhere any more, and we should analyze the polarization of a wave propagating at a general angle ψ to the background magnetic field. Defining the \mathbf{z} axis to be parallel to the wave vector \mathbf{k} and the \mathbf{x} axis perpendicular to the background magnetic field, we obtain an orthogonal frame $(\mathbf{x}, \mathbf{y}, \mathbf{z})$. In this frame, the transverse components of the two characteristic waves can be written as [23]

$$\frac{E_x}{E_y} = -i \frac{Y \sin^2 \psi}{2(1-X) \cos \psi} \pm i \left[1 + \frac{Y^2 \sin^4 \psi}{4(1-X)^2 \cos^2 \psi} \right]^{1/2}. \quad (9)$$

In Eq. (9), X and Y are defined respectively as

$$X = \frac{\omega_{pe}^2}{\omega^2} \quad \text{and} \quad Y = \frac{\Omega_e}{\omega}, \quad (10)$$

where ω is the wave's frequency, ω_{pe} is the electron plasma frequency, and Ω_e is the electron gyrofrequency. If the wave propagates quasi-parallel to the background field, *i.e.*, $\sin \psi \ll 1$ and $\cos \psi \sim 1$, we have

$$\frac{Y \sin^2 \psi}{2(1-X) \cos \psi} \approx 0. \quad (11)$$

Equation (9) then becomes

$$\frac{E_x}{E_y} \approx \pm i, \quad (12)$$

which means the characteristic waves can be taken as circularly polarized for quasi-parallel propagation. On the other hand, for high frequency EM waves satisfying $\omega \gg \Omega_e$, we have $Y \ll 1$. As long as the propagation direction is not too close to the perpendicular direction, *i.e.*, $\cos \psi$ is not small enough to break Eq. (11), Eq. (12) still holds. In this situation, the analysis of the Faraday effect based on circularly polarized characteristic waves is still valid. As pointed out in Ref. [24], in a real polarimetric system, the Cotton-Mouton effect and the Faraday effect co-exist. However, the existence of the Cotton-Mouton effect does not invalid the existence of the Faraday effect. The Faraday effect can be measured even when the wave

becomes elliptically polarized. Indeed, both effects can be used as diagnostic tools [24]. As long as the Faraday effect can be measured, it is valid to discuss the dynamical phase and the geometric phase of the Faraday rotation angle.

DeMarco and Segre studied the polarization of an EM wave with a wave vector that has a component perpendicular to the background magnetic field using the WKB approximation [29]. They proved that linearly polarized waves propagating in general direction can remain linearly polarized. They also suggested that the Faraday rotation can be used to measure the poloidal magnetic field in tokamaks, which has been experimentally verified [31]. According to their results, for a linearly polarized wave propagating in general direction, the dynamical Faraday rotation angle, which depends on the local dispersion relations of the circularly polarized characteristic waves, takes the form of

$$\theta_{Fd} = 2.5 \times 10^{-17} \lambda^2 \int_P n(\mathbf{r}) B_r(\mathbf{r}) dr , \quad (13)$$

where λ denotes the wavelength, B_r is the component of background magnetic field along the wave propagation direction, the integral path P is the wave trajectory, and this formula is expressed in Gaussian units.

To represent the wave's polarization, a frame sitting in the polarization surface is required. Since the wave's polarization surface varies from place to place, there exists no global reference frames. A set of local frames have to be chosen to describe the wave's polarization orientations. We choose two orthogonal unit vectors \mathbf{e}_1 and \mathbf{e}_2 within the polarization surface and a third unit vector \mathbf{e}_3 perpendicular to them, satisfying $\mathbf{e}_1 \times \mathbf{e}_2 = \mathbf{e}_3$. Then, for circularly polarized characteristic waves, the dynamical part of wave vector \mathbf{k}_d is along \mathbf{e}_3 . The complex amplitude $\tilde{\mathbf{E}}(\mathbf{r})$ in Eq. (4) can be expressed as

$$\tilde{\mathbf{E}} = \tilde{E}_\perp (\mathbf{e}_1 \pm i\mathbf{e}_2) , \quad (14)$$

where the “+” denotes the right circularly polarized wave and the “−” denotes the left circularly polarized one.

Combining Eqs. (6)-(8) and (14), we can solve for the geometric wave vector \mathbf{k}_g to the order of $O(\varepsilon)$. It satisfies the relation

$$\mathbf{k}_g \cdot \mathbf{e}_k = \mp \left(\nabla \mathbf{e}_2 \cdot \mathbf{e}_1 + \frac{1}{2} \nabla \times \mathbf{e}_3 \right) \cdot \mathbf{e}_k , \quad (15)$$

where \mathbf{e}_k is the unit vector along the \mathbf{k} direction. The difference between \mathbf{e}_k and \mathbf{e}_3 is small, *i.e.*, $|\mathbf{e}_k - \mathbf{e}_3|$ is of order ε . This shows that the electric field perturbation, the magnetic

field perturbation, and the wave vector are no longer perpendicular to each other exactly because of the nonuniformity of the magnetized plasmas, though the deviation is very small. We note that \mathbf{k}_g is called the geometric wave vector because of its geometric origin. It's easy to observe that the \mathbf{k}_g depends the spatial variations of the local frame instead of the dispersion relations. Obviously, $k_g/k_d \sim O(\varepsilon)$.

The circularly polarized wave's phase can then be expressed as

$$\theta = \theta_d + \theta_g = \left(\int_P \mathbf{k}_d \cdot d\mathbf{r} - \omega t \right) + \int_P \mathbf{k}_g \cdot d\mathbf{r} , \quad (16)$$

where the integral path P is the wave trajectory. The dynamical phase θ_d depends on the wave's local dispersion relation along its trajectory, which is well-known. The additional geometric phase θ_g is of our interest. To study the geometric phase in more detail, we further divide it into two parts

$$\theta_g = \int_P \mathbf{k}_g \cdot d\mathbf{r} = \theta_{gI} + \theta_{gII} , \quad (17)$$

$$\theta_{gI} = \mp \int_P d\mathbf{e}_2 \cdot \mathbf{e}_1 , \quad (18)$$

$$\theta_{gII} = \mp \frac{1}{2} \int_P (\nabla \times \mathbf{e}_3) \cdot d\mathbf{r} . \quad (19)$$

Here, θ_{gI} and θ_{gII} are named type-I and type-II geometric phase respectively.

We emphasize that the two circularly polarized waves' trajectories are close to each other only guarantees that their integral paths P are the same. It doesn't mean that \mathbf{k}_g have to be the same. Indeed, their \mathbf{k}_g depend only on the behavior of \mathbf{k}_d along their trajectories, but they depend on \mathbf{k}_d through different function forms. According to Eq. (15), \mathbf{k}_g for right and left circularly polarized waves have the same magnitude but different signs.

It's easy to see from Eq. (18) that θ_{gI} depends on \mathbf{e}_1 and \mathbf{e}_2 , while there is a freedom to choose local reference frames because they can rotate freely within the plane perpendicular to \mathbf{e}_3 . The definition of local frames is actually a choice of gauge. We choose a specific gauge as follows

$$\mathbf{e}_1 = \frac{k_z}{k\sqrt{k_x^2 + k_y^2}} (k_x \mathbf{e}_x + k_y \mathbf{e}_y - \frac{k_x^2 + k_y^2}{k_z} \mathbf{e}_z) , \quad (20)$$

$$\mathbf{e}_2 = \frac{1}{\sqrt{k_x^2 + k_y^2}} (-k_y \mathbf{e}_x + k_x \mathbf{e}_y) , \quad (21)$$

where (k_x, k_y, k_z) are three components of \mathbf{k}_d , \mathbf{e}_x , \mathbf{e}_y , and \mathbf{e}_z are unit vectors in \mathbf{x} , \mathbf{y} and \mathbf{z} direction respectively, and $k_d = \sqrt{k_x^2 + k_y^2 + k_z^2}$ is the magnitude of the dynamical wave vector. This gauge keeps \mathbf{e}_2 within the \mathbf{x} - \mathbf{y} plane. Under this gauge, the type-I geometric phase is

$$\theta_{gI} = \pm \int_P \frac{k_z(k_x dk_y - k_y dk_x)}{k_d(k_x^2 + k_y^2)}. \quad (22)$$

If the evolving path of \mathbf{k}_d in the parameter space forms a closed loop, *i.e.*, the polarization surface returns to its original direction after the wave travels some distance, then the Stokes theorem can be applied to Eq. (22) to obtain

$$\begin{aligned} \theta_{gI}(\tau) &= \pm \iint_S \frac{k_x dk_y dk_z + k_y dk_z dk_x + k_z dk_x dk_y}{k^3} \\ &= \pm \iint_S \frac{\mathbf{k} \cdot d\mathbf{S}_k}{k^3}, \end{aligned}$$

which equals exactly the solid angle spanned by the integral path in the parameter space of \mathbf{k}_d (see Fig. 2). The value of θ_{gI} obviously depends on the choice of gauge. However, if the polarization surface returns to its initial direction, it can be proved that different gauges only bring differences of integer multiples of 2π to θ_{gI} , which has no observable effects. The path dependence of type-I geometric phase shows that the wave phase is not a single-value function of position \mathbf{r} . It relies on the trajectory of the wave.

On the other hand, θ_{gII} is gauge-invariant because it depends only on \mathbf{e}_3 and has nothing to do with the gauge choice. The polarization surface of the wave may rotate slightly because of the spatially nonuniformity of the background magnetic field. In this non-inertial reference frame, the rotation of the polarization surface provides a centrifugal force on the oscillating plasma. The centrifugal force has the same period as the plasma oscillation, and generates an extra phase, *i.e.*, the type-II geometric phase, to the plasma waves. It is interesting to note that the gyrophase of charged particles moving in spatially non-uniform magnetic field also manifests the type-II geometric phase similarly. Let's consider the gyromotion of a charged particle in a spatially non-uniform background magnetic field. Let \mathbf{b} be the unit vector along the background field. The particle rotates in the gyro-surface perpendicular to the background field. We choose two other unit vectors \mathbf{e}_1 and \mathbf{e}_2 satisfying $\mathbf{b} = \mathbf{e}_1 \times \mathbf{e}_2$ to form the local frame. Particle's velocity \mathbf{v} can be expressed as $\mathbf{v} = v_{\parallel} \mathbf{b} + v_{\perp} (\cos \theta \mathbf{e}_1 + \sin \theta \mathbf{e}_2)$, where v_{\parallel} is the parallel velocity, v_{\perp} is the perpendicular velocity, and θ is the gyrophase. However, the direction of the background field may change during each gyro period as the

particle moves. The gyro-surface will rotate with the angular velocity $\boldsymbol{\Omega} = \mathbf{b} \times \dot{\mathbf{b}}$. In this non-inertial frame, there is a centrifugal force on the particle, which provides an extra acceleration $\mathbf{a} = -\boldsymbol{\Omega} \times \mathbf{v}$. This acceleration thus generates an extra angular velocity to particle's gyromotion, $\dot{\theta}_{extra} = -v_{\parallel}/v_{\perp} \cdot \dot{\mathbf{b}} \cdot (-\sin\theta\mathbf{e}_1 + \cos\theta\mathbf{e}_2)$. Averaging over one period, we have $d\theta_{extra} = -1/2 \cdot (\nabla \times \mathbf{b}) \cdot d\mathbf{r}_{\parallel}$, which is exactly the type-II geometric phase for the EM waves given by Eq. (19).

We note that there are differences in both dynamical and geometric phases between right and left circularly polarized waves along (approximately) the same trajectory. These differences are manifested as the Faraday rotation. A linearly polarized wave is the superposition of a right and a left circularly polarized waves,

$$\begin{aligned} \mathbf{E}_{linear} &= \tilde{\mathbf{E}}_R e^{i\theta_R} + \tilde{\mathbf{E}}_L e^{i\theta_L} \\ &= E_{\perp}(\mathbf{e}_1 + i\mathbf{e}_2)e^{i\theta_R} + E_{\perp}(\mathbf{e}_1 - i\mathbf{e}_2)e^{i\theta_L} \\ &= 2E_{\perp} \left(\cos \frac{\theta_L - \theta_R}{2} \mathbf{e}_1 + \sin \frac{\theta_L - \theta_R}{2} \mathbf{e}_2 \right) e^{i \frac{\theta_L + \theta_R}{2}}, \end{aligned}$$

which shows that the angle between the polarization orientation and \mathbf{e}_1 , *i.e.*, the Faraday rotation angle, is

$$\theta_F = \frac{\theta_L - \theta_R}{2}, \quad (23)$$

and the phase of the wave is

$$\theta_{linear} = \frac{\theta_L + \theta_R}{2}. \quad (24)$$

Because θ_g has opposite signs for the right and left circularly polarized waves, it contributes to the Faraday rotation angle θ_F but not to the phase θ_{linear} , while the dynamical phase contributes to both. The Faraday rotation angle then takes the form of

$$\theta_F = \theta_{Fd} + \theta_{Fg}, \quad (25)$$

where the dynamical phase θ_{Fd} depends on the difference between the dispersion relations of the right and left circularly polarized waves, and the geometric phase θ_{Fg} can be expressed as

$$\theta_{Fg} = \int_P d\mathbf{e}_1 \cdot \mathbf{e}_2 - \frac{1}{2} \int_P (\nabla \times \mathbf{e}_3) \cdot d\mathbf{r}. \quad (26)$$

The first term on the right-hand side is the type-I geometric rotation angle θ_{FgI} , and the second term is the type-II geometric rotation angle θ_{FgII} .

To calculate the geometric phase, the integral path P should be specified. It is determined by the ray-tracing equation

$$\frac{d\mathbf{r}}{dt} = \frac{\partial\omega(\mathbf{k}_d, \mathbf{r})}{\partial\mathbf{k}_d}. \quad (27)$$

The evolution of the dynamical wave vector \mathbf{k}_d is described by

$$\frac{d\mathbf{k}_d}{dt} = -\frac{\partial\omega(\mathbf{k}_d, \mathbf{r})}{\partial\mathbf{r}}. \quad (28)$$

The expression of $\omega(\mathbf{k}_d, \mathbf{r})$ can be obtained from Eq. (8) according to the profiles of the magnetized plasma.

We now evaluate the influence of the geometric phase to the Faraday rotation angle measurement, since it is an important technique for plasma diagnostics. The wave's frequency in Faraday rotation diagnostics are commonly very high, which implies that the variation of the polarization surface is small. To compare the magnitude of the geometric Faraday rotation angle θ_{Fg} with that of the dynamical Faraday rotation angle θ_{Fd} , we consider their ratios to the dynamical phase θ_d of the circularly polarized characteristic wave. For circularly polarized waves, the ratio between the geometric phase and the dynamical phase θ_g/θ_d is of order ε . According to Eq. (23), $\theta_{Fg} = (\theta_{Lg} - \theta_{Rg})/2$, where the geometric phase of the left and right circularly polarized waves, θ_{Lg} and θ_{Rg} , have the same magnitude but opposite signs, that is $\theta_{Lg} = -\theta_{Rg} = \theta_g$. Thus $\theta_{Fg} = \theta_g$ holds, and the ratio θ_{Fg}/θ_d is also of order ε . For the 0.89THz FIR wave used in a typical polarimetric system (as in Ref. [31]), the wave length λ is about $3 \times 10^{-4}m$. While in real devices the typical scale of nonuniformity L is 1m [34, 35]. The value of $\varepsilon \equiv \lambda/L$ is 10^{-4} , which means that $\theta_{Fg}/\theta_d = O(\varepsilon) \sim 10^{-4}$. According to Eq. (13), the ratio between the dynamic Faraday angle θ_{Fd} and θ_d can be estimated as

$$\frac{\theta_{Fd}}{\theta_d} \approx 4 \times 10^{-14} \lambda^3 n_e B_r, \quad (29)$$

where all the quantities are in SI unit. Given $n_e = 10^{20}/m^3$, $B_r = 2T$, and $\lambda = 3 \times 10^{-4}m$, we obtain $\theta_{Fd}/\theta_d \approx 2 \times 10^{-4}$. Therefore

$$\frac{\theta_{Fg}}{\theta_{Fd}} = \frac{\theta_{Fg}/\theta_d}{\theta_{Fd}/\theta_d} \sim \frac{10^{-4}}{2 \times 10^{-4}} = O(1), \quad (30)$$

which indicates that the magnitudes of geometric and dynamical Faraday rotation angles are of the same order. Though the order comparison is only a rough estimation, it nevertheless shows that the contribution from the geometric phase to the Faraday rotation angle can be significant in certain situations.

The gauge-dependent property of the geometric phase also brings difficulty to the measurement of the Faraday rotation angle. When measuring polarization direction in different polarization surface, different gauge choice may give different result. Two observers should specify their gauge choices and the relation between their gauges to compare their experimental results.

Different parts of the Faraday rotation angle have different properties. The dynamical part depends on wave's frequency, the background field, and the properties of the plasma, while the geometric part has nothing to do with wave's frequency and only depends on the spatial geometric structure of the wave vector. When diagnosing plasmas with Faraday rotation, if we can separate the geometric Faraday rotation angle from the dynamical one, then the geometric phase can be experimentally observed, which can be used to improve the diagnostic accuracy. One method to separate them is to utilize the dependence of the dynamical Faraday rotation angle on the frequency of the probing wave (see Fig. 3). Another method is to employ two waves with same frequency and trajectory but opposite directions (see Fig. 4). In addition, the fact that the phase of linearly polarized wave θ_{linear} contains only dynamical phase [see Eq. (24)], can be utilized. The existence of the geometric Faraday rotation angle brings in extra complexity to applications of the Faraday effect in plasma diagnostics. However, realizing its existence and understanding its unique properties can help to improve the measurement accuracy and develop new diagnostic techniques. There are other possible error sources in Faraday rotation experiments, such as depolarization of the probing beam due to the perpendicular gradients of electron density, temperature, velocity, and absorption anisotropy of the EM waves [36]. We will consider these effects in future studies.

* This research is supported by the China Scholarship Council (2009601134), ITER-China Program (2010GB107001), the National Natural Science Foundation of China (NSFC-11075162), and the U.S. Department of Energy (DE-AC02-09CH11466). Jian Liu thanks the Theory Department of Princeton Plasma Physics Laboratory for the hospitality during his visit.

[1] D. Chruściński and A. J. kowski, *Geometric phases in classical and quantum mechanics* (Birkhauser, 2004).

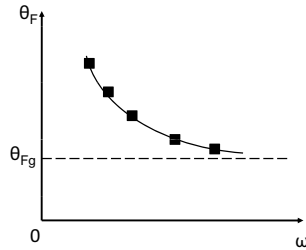


FIG. 3. Faraday rotation angle θ_F as a function of the wave frequency ω . Since the geometric phase θ_{Fg} doesn't depend on ω , the value of θ_F approaches that of θ_{Fg} at the limit of $\omega \rightarrow \infty$. This dependence can be used to separate θ_{Fg} from θ_F .

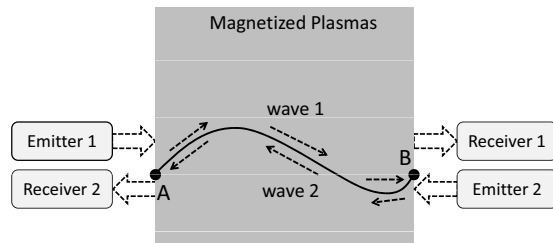


FIG. 4. Wave 1 and 2 have the same frequency and trajectory but opposite directions. After propagating through the plasma, their Faraday rotation angles θ_{F1} and θ_{F2} can be measured. Their geometric rotation angles θ_{Fg1} and θ_{Fg2} are the same, but dynamical rotation angles θ_{Fd1} and θ_{Fd2} have opposite signs. Therefore θ_{Fg} and θ_{Fd} can be separated as $\theta_{Fg1} = \theta_{Fg2} = (\theta_{F1} + \theta_{F2})/2$ and $\theta_{Fd1} = -\theta_{Fd2} = (\theta_{F1} - \theta_{F2})/2$.

- [2] J. Anandan, *Nature* **360**, 307 (1992).
- [3] M. V. Berry, *Proc. R. Soc. Lond. A* **392**, 45 (1984).
- [4] M. V. Berry, *J. Phys. A: Math. Gen.* **18**, 15 (1989).
- [5] M. V. Berry, "The quantum phase, five years after," (*Geometric Phases in Physics*, edited by A. Shapere and F. Wilczek, World Scientific, Singapore, 1989) pp. 1–28.
- [6] A. Mostafazadeh and A. Bohm, *J. Phys. A: Math. Gen.* **26**, 5473 (1993).
- [7] J. Ren, P. Hänggi, and B. W. Li, *Phys. Rev. Lett.* **104**, 170601 (2010).
- [8] Y. Kohmura, K. Sawada, and T. Ishikawa, *Phys. Rev. Lett.* **104**, 244801 (2010).
- [9] P. J. Leek, J. M. Fink, A. Blais, R. Bianchetti, M. Göppl, J. M. Gambetta, D. I. Schuster, L. Frunzio, R. J. Schoelkopf, and A. Wallraff, *Science* **318**, 1889 (2007).
- [10] E. Sjöqvist, *Physics* **1**, 35 (2008).

- [11] K. Fujikawa and M. G. Hu, Phys. Rev. A **79**, 052107 (2009).
- [12] J. Boer, K. Papadodimas, and E. Verlinde, Phys. Rev. Lett. **103**, 131301 (2009).
- [13] C. A. Mead, Rev. Mod. Phys. **64**, 51 (1992).
- [14] G. Falci, R. Fazio, G. M. Palma, J. Siewert, and V. Vedral, Nature **407**, 355 (2000).
- [15] A. Kuppermann and Y. M. Wu, Chem. Phys. Lett. **205**, 577 (1993).
- [16] A. Tomita and R. Y. Chiao, Phys. Rev. Lett. **57**, 937 (1986).
- [17] L. Sptizer, Phys. Fluids **1**, 253 (1958).
- [18] J. H. Hannay, J. Phys. A: Math. Gen. **18**, 221 (1985).
- [19] B. Simon, Phys. Rev. Lett. **51**, 2167 (1983).
- [20] R. G. Littlejohn, Phys. Rev. A **38**, 6034 (1988).
- [21] A. Bhattacharjee, G. M. Schreiber, and J. B. Taylor, Phys. Fluids B **4**, 2737 (1992).
- [22] J. Liu and H. Qin, Phys. Plasmas **18**, 072505 (2011).
- [23] I. H. Hutchinson, *Principles of Plasma Diagnostics* (Cambridge University Press, 2002).
- [24] S. E. Segre, Plasma Phys. Control. Fusion **41**, R57 (1999).
- [25] S. E. Segre, J. Opt. Soc. Am. A **17**, 1682 (2000).
- [26] H. Soltwisch, Rev. Sci. Instrum. **57**, 1939 (1986).
- [27] J. A. Stamper and B. H. Ripin, Phys. Rev. Lett. **34**, 138 (1975).
- [28] S. Mancuso and S. R. Spangler, Astrophys. J. **525**, 195 (1999).
- [29] F. DeMarco and S. E. Segre, Plasma Phys. **14**, 245 (1972).
- [30] F. Hofmann and G. Tonetti, Nucl. Fusion **28**, 1871 (1988).
- [31] W. Kunz and E. TFR, Nucl. Fusion **18**, 1729 (1978).
- [32] T. D. Stix, *Waves in Plasmas* (American Institute of Physics, 1992).
- [33] S. M. Rytov, Dokl. Akad. Nauk SSSR **31**, 263 (1938).
- [34] M. Shimada and et al., Nucl. Fusion **47**, S1 (2007).
- [35] H. Q. Liu and et al., Plasma Phys. Control. Fusion **49**, 995 (2007).
- [36] G. S. Sarkisov, Quantum Electronics **26**, 799 (1996).

The Princeton Plasma Physics Laboratory is operated
by Princeton University under contract
with the U.S. Department of Energy.

Information Services
Princeton Plasma Physics Laboratory
P.O. Box 451
Princeton, NJ 08543

Phone: 609-243-2245
Fax: 609-243-2751
e-mail: pppl_info@pppl.gov
Internet Address: <http://www.pppl.gov>